

Network Modelling of Criminal Collaborations with Dynamic Bayesian Steady Evolutions

F.O. Bunnin ^{*} A. Shenvi ^{†*} J.Q. Smith ^{‡*}

Abstract

The threat status and criminal collaborations of potential terrorists are hidden but give rise to observable behaviours and communications. Terrorists, when acting in concert, need to communicate to organise their plots. The authorities utilise such observable behaviour and communication data to inform their investigations and policing. We present a dynamic latent network model that integrates real-time communications data with prior knowledge on individuals. This model estimates and predicts the latent strength of criminal collaboration between individuals to assist in the identification of potential cells and the measurement of their threat levels. We demonstrate how, by assuming certain plausible conditional independences across the measurements associated with this population, the network model can be combined with models of individual suspects to provide fast transparent algorithms to predict group attacks. The methods are illustrated using a simulated example involving the threat posed by a cell suspected of plotting an attack.

Keywords: chain event graphs, dynamic non-Gaussian models, Markov processes, probabilistic graphical models, terrorist networks, statistical network models, decision support systems

1 Introduction

In Bunnin and Smith (2019) we showed how to build a Bayesian dynamic model that could help police monitor and frustrate lone criminals in perpetrating acts of violence against the general public. However it is well known that such criminals often act in gangs that co-ordinate themselves so as to present a much more severe threat. Performing this multivariate extension of the above technologies is far from straightforward. It requires bespoke graphically supported probabilistic models of teams of criminals over a given population cooperating in a way that leads to an attack cell. This type of model then needs to be combined in a coherent way with models we have of the individuals within that population. In

^{*}The Alan Turing Institute, British Library, 96 Euston Road, London NW1 2DB

[†]Centre for Complexity Science, University of Warwick, Coventry, CV4 7AL

[‡]Department of Statistics, University of Warwick, Coventry, CV4 7AL

this paper we develop a new class of models that is able to do this. The system is flexible enough to implement change-points, and interventions to the system in real time. Furthermore as far as is possible our inferences are driven by closed form recurrences meaning that the method computes forecasts quickly in real time and its inference is scalable to much larger networks. The class of models we propose here is to our knowledge entirely new. The proposed methodology provides as outputs various evocative graphs and figures that communicate the outputs of the model to give real time decision support to the Bayesian decision maker. The methodology and these outputs are illustrated in simulated example based on real domain information.

1.0.1 Background and context

Identification and disruption of the activities of terrorist networks is a prime objective of police and security services (Allen and Dempsey, 2018; Europol, 2018). This comes with several challenges: terrorists usually hide or disguise their intentions and activities; personal communications are private and are often encrypted, and the numbers and powers of the policing authorities are rightly limited in democratic societies. However, terrorists *do* need to perform certain activities and to communicate in order to organise and execute attacks. These activities and communications give rise to observable data that in conjunction with domain knowledge can be used to construct statistical models to aid prevention and disruption of attacks.

Under current legislation, when justified and after due legal process, policing authorities can monitor the activities and intercept the communications of individuals in order to protect public safety (Investigatory Powers Act. (c.25), 2016). Every week hundreds of new leads arise in the form of partial and fragmentary information (Anderson, 2016). Investigating bodies must decide how to use the limited resources available to them to prioritise and de-prioritise cases according to the regularly incoming noisy leads (BBC, 2019).

Bunnin and Smith (2019) presented a Bayesian hierarchical model for the progression of an individual terrorist suspect’s threat status based on streaming data, hereafter called the **Radicalisation and Violent Extremism (RVE)** model. In this paper we present a Bayesian methodology to integrate knowledge on individual suspects and incoming real-time leads into a dynamic weighted network model. The weights of this network model are informed by an underlying *dynamic steady model*. We call this methodology the **criminal collaboration model**. Each such network is composed of individuals¹ as vertices. An edge between two individuals indicates a potential **conspiratorial link** between them. The weight on the edge is a statistical distribution indicating the strength of this link. Such links between individuals are informative of potential joint attacks. Additionally, we demonstrate how an **integrated decision support system** can be obtained by combining the dynamic network data with the RVE models of the members of the terrorist population under consideration. This

¹persons of intelligence interest

allows us to then define suitable **cell-based threat measures** to estimate the cells’ current and future threat distributions by considering the threat posed by the members of the cell, and the activities of the cell as a whole.

Thus we present a network methodology that is customised to the prevention of terrorist attacks through the use of domain knowledge and data available to the counter-terrorism authorities. Note that it is essential in this domain that whatever methodology we choose to use is simple, explainable, interpretable and can be used with real-time data. This allows the model to be adapted as needed and also ensures transparency in its workings given the sensitive nature of this domain.

1.0.2 Related research

The structure, scope, dynamics and intent of such criminal networks can be very diverse, and using statistical network methods to analyse these is a very active area of research (Krebs, 2002; Morselli, 2009; Helfstein and Wright, 2011; Berlusconi et al., 2016; Remmers, 2019). The formal use of network data for intelligence use has a long history going back to at least World War II when “Traffic Analysis”² was used by the allied forces (Meter, 2002; Cunningham et al., 2015).

In the context of academic terrorism research, network modelling was originally assessed by Sparrow (1991). Sparrow considered the utility of various network centrality concepts applied to criminal intelligence including *betweenness*, *point strength*, and *business*. Since then the social network aspects of terrorist networks have been researched extensively utilising diverse methods. These include centrality measures to identify key individuals and heterogeneous roles (Toth et al., 2013), Bayesian bipartite graph methods to identify overlapping cells (Ranciati et al., 2017), multipartite graph methods to cluster similar terrorist groups (Campedelli et al., 2019), and dynamic line graphs to visualise the temporal dynamics of terrorist actors in covert actions and events (Broccatelli et al., 2016).

The existing terrorist network research, however, does not focus on the types of real-time data that the authorities have access to. Nor does it utilise the formal structure of stochastic processes that we assume for the underlying trajectories of the individual suspects and their collaboration levels. Thus we believe our contribution to this field is both novel and of utility to the policing authorities.

1.0.3 Model requirements

It is essential that our model is dynamic and supports an open population. Firstly, individuals enter (*immigration*) and leave (*emigration*) the pool of monitored suspected criminals at each time point. Immigration is through new leads

²A 1948 US Army manual defines Traffic Analysis as “the study of the external characteristics of signal communications” and states that it is used for “drawing deductions and inferences of value as intelligence even in the absence of specific knowledge of the contents of the message” (US Department of the Army, 1948).

that have passed a triage process³. Emigration may occur due to various reasons. These include death, arrest, evidence of innocence, physical movement to leave the jurisdiction of the authorities, or de-prioritisation based on evidence and case load. In network terminology these are node additions and deletions. Secondly, to capture the changing strengths of the conspiratorial link between individuals, it is also essential that the edge weights in our model are dynamic and responsive to evidence.

Other important features of a criminal network model noted by Sparrow (1991) are incompleteness, fuzzy boundaries and the importance of weak ties. Individuals will, often successfully, hide their existence, behaviour and communications. In statistical network terminology, nodes and edges will be missing not at random (Rubin, 1976). Within this context of incomplete knowledge and uncertainty, the fluidity of the processes and the necessity for external often surprising information to be accommodated into the description of the process makes the adoption of Bayesian methodologies attractive if not essential.

1.0.4 Model overview

Our Bayesian criminal collaboration model was designed keeping these requirements in mind. A high-level structural representation of the model is given in Figure 1 (see Section 3 for details).

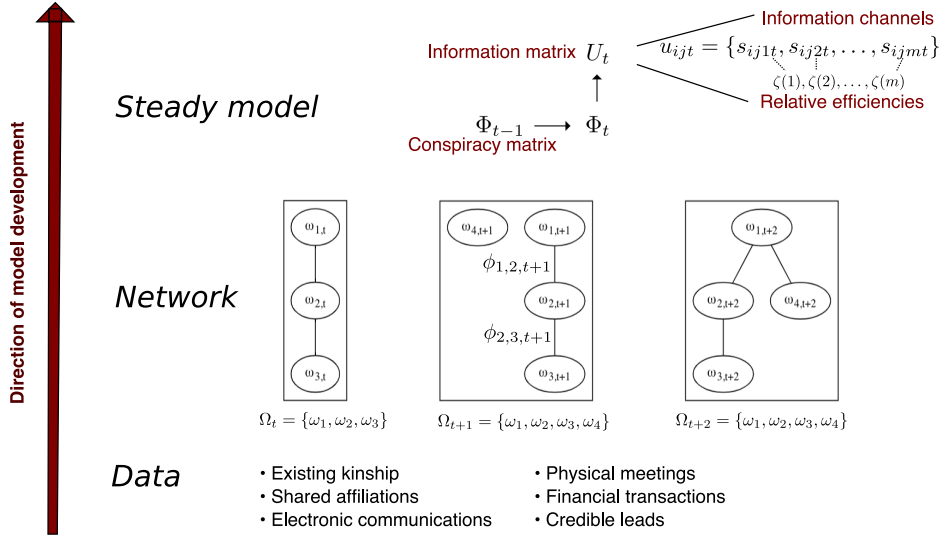


Figure 1: Overview of the criminal collaboration model.

Existing information and incoming real-time observations data collected

³See Section 3.1 for details.

from various information channels such as direct monitoring, information obtained from other agencies or informants, and financial transactions are used to identify the pool of individuals monitored at time t . This data determines which edges should be added to the network from time $t - 1$ to indicate new connections. The strength of the conspiratorial link on the edges of the network are estimated using a steady model. The steady model can be graphically depicted by a compact dynamic Bayesian network (DBN) as shown in Figure 1.

We find that a Bayesian conjugate Gamma-Poisson steady model works well for our application and facilitates real-time implementation across a potentially very large number of connections. Note that other distributions can be used if appropriate for the specific application (West and Harrison, 1997; Smith, 1979, 1981). The criminal collaboration model at time t is then combined with the individual RVE models of the members of the monitored suspected criminals pool at time t . Under a set of assumptions, we can then utilise this integrated decision support system (IDSS) to obtain a cell-based threat measure for a group of individuals suspected to be working together within a criminal cell. The Bayesian paradigm provides the ideal framework for composing two dynamic models of different aspects of a process into a single coherent composite combining together.

Thus, in contrast to the majority of existing terrorist network research:

- i) we have a formal stochastic model for the threat state of individuals informed by a Bayesian hierarchical model linking states, tasks and data; these form the nodes of the network;
- ii) our population is conceptually defined by concrete periodic policing decisions; these define the open population immigration and emigration;
- iii) ties between individuals are modelled by latent conspiratorial links informed by observable data and prior information; these form the edges of the network;
- iv) we utilise a Bayesian paradigm to combine individual processes and the multivariate network process;
- v) our focus is on predicting and disrupting real-time terrorist activity.

The paper is organised as follows: Section 2 summarises the individual RVE model introduced in Bunnin and Smith (2019) which provides context for our collaboration model presented in Section 3. Section 3 further demonstrates how a conjugate Gamma-Poisson steady model can be used to estimate the latent conspiratorial links which form the edge weights in the networks of the collaboration model. In Section 4 we show how the collaboration model and the individual RVEs can be combined to create an IDSS. Further, we demonstrate how the IDSS can be used to create suitable cell-level threat measures which can aid in prioritising and de-prioritising cases. In Section 5 we present the deployment of the model to simulated data informed by real cases in the public domain, and we conclude with a discussion of the results and future work in Section 6.

2 The individual RVE model

The individual RVE model developed in Bunnin and Smith (2019) hypothesised for a potential criminal the probabilistic relationship at time t between:

- The latent threat state $W_t \in \{w_0 \dots w_k\}$ of a potential criminal;
- Normally hidden tasks $\theta_t = \{\theta_{1t}, \dots, \theta_{dt}\}$ that the criminal may be engaged in to carry out a certain plot;
- Observable data \mathbf{Y}_t resulting from task engagement.

The Bayesian hierarchical RVE model uses as input the observable noisy data to output a vector $\boldsymbol{\pi}_t = \{\pi_{1t}, \dots, \pi_{kt}\}$ where π_{it} indicates the probability of the suspect being in threat state w_i at time t . At the deepest level of the hierarchy, a graphical model called the Reduced Dynamic Chain Event Graph (RDCEG) is used to model the threat states (Smith and Shenvi, 2018; Shenvi and Smith, 2019). In this application the RDCEG can be represented as a finite state semi-Markov process. For each criminal plot, we can identify a set of tasks which are indicative of the progression of the suspect’s efforts towards enacting the plot. The vector θ_t lies in the middle layer of the RVE hierarchical model and provides indicators of which of these tasks the suspect is engaging in at time t . The observed data \mathbf{Y}_t is transformed into a \mathbb{R}^d -valued signal \mathbf{Z}_t which indicates the intensities with which the various tasks are being carried out at time t . The j th component of \mathbf{Z}_t uses the relevant subset of the data \mathbf{Y}_t to produce the task intensity for task θ_{jt} . An example of the threat state space, tasks and observable variables for a vehicle, knife, gun or bomb attack is provided in Table 4 in Appendix C of the supplementary material (Bunnin et al., 2020).

Consider an RVE model of a lone attacker. A general template for such an attack is described by the graph of the RDCEG in Figure 2. The state space of this model is represented by the vertices of this graph and the edges represent the possible transitions between the states.

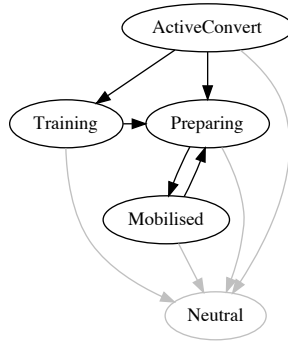


Figure 2: RDCEG graph of an RVE model of a lone attacker

| M^0 | Neutral | ActiveConvert | Training | Preparing | Mobilised |
|------------|-------------------------|----------------------|-------------------------|-------------------------|-------------------------|
| N | 0 | 0 | 0 | 0 | 0 |
| A | $m_{a,n}$ | 0 | $m_{a,t}$ | $m_{a,p}$ | 0 |
| T | $m_{t,n}$ | 0 | 0 | $m_{t,p}$ | 0 |
| P | $m_{p,n}$ | 0 | 0 | 0 | $m_{p,m}$ |
| M | $m_{m,n}$ | 0 | 0 | $m_{m,p}$ | 0 |
| $M(t, t')$ | Neutral | ActiveConvert | Training | Preparing | Mobilised |
| N | 1 | 0 | 0 | 0 | 0 |
| A | $\zeta_a(t, t')m_{a,n}$ | $1 - \zeta_a(t, t')$ | $\zeta_a(t, t')m_{a,t}$ | $\zeta_a(t, t')m_{a,p}$ | 0 |
| T | $\zeta_t(t, t')m_{t,n}$ | 0 | $1 - \zeta_t(t, t')$ | $\zeta_t(t, t')m_{t,p}$ | 0 |
| P | $\zeta_p(t, t')m_{p,n}$ | 0 | 0 | $1 - \zeta_p(t, t')$ | $\zeta_p(t, t')m_{p,m}$ |
| M | $\zeta_m(t, t')m_{m,n}$ | 0 | 0 | $\zeta_m(t, t')m_{m,p}$ | $1 - \zeta_m(t, t')$ |

Table 1: The two matrices show the semi-Markov transition matrix $M(t, t')$ and the transition matrix M^0 of its embedded Markov chain.

The **Neutral** state, w_0 , is the sole absorbing state that, by definition, can be reached from any other state and is thus usually not depicted in the graph of the RDCEG (see Shenvi and Smith (2019) for details of an RDCEG model). Intuitively, we can think of the **Neutral** state not being essential to depict as a transition to the neutral state indicated de-prioritisation of this individual’s case. The parameters associated with the **Neutral** state can, if needed, be estimated from the underlying statistical model. The remaining states $\{w_i\}_{i=1}^4$ are labelled as **{ActiveConvert, Training, Preparing, Mobilised}**. These non-absorbing states are known as the *positions* of the RDCEG.

The prior state probabilities, the edge probabilities and the holding time distributions are constructed from expert judgement. The format of the latter two are shown in Table 1. Matrix M^0 contains the edge probabilities p_{ij} , i.e. the probabilities of moving from state i to state j given a transition has occurred. Matrix $M(t, t')$ is the full transition matrix which is the product of the edge probability and the state dependent holding time distribution ζ for a small time interval (t, t') .

The position probabilities are updated using the following recurrence:

$$p(W_t = w_i | \mathbf{Z}_{t-1}) = \sum_{w_j} p(W_{t-1} = w_j | \mathbf{Z}_{t-1}) M_{j,i}(t-1, t, M^0, \zeta) \quad (1)$$

$$p(W_t = w_i | \mathbf{Z}_t) \propto p(W_t = w_i | \mathbf{Z}_{t-1}) \times \sum_{\theta \in \boldsymbol{\theta}_t} p(\mathbf{Z}_t | \theta) p(\theta | W_t = w_i) \quad (2)$$

Equation (1) updates the posterior at time $t-1$ to the prior at time t through the semi-Markov transition matrix. Equation (2) updates the prior at time t to the posterior at time t once the signal \mathbf{Z}_t is inferred from the observed data \mathbf{Y}_t . Inference works from observable data through task intensities to combine with the task likelihoods and the predefined probabilities of tasks given states. The

recurrences thus allow periodic updating of the posterior state probabilities at each time t . Moreover direct intelligence gained that a suspect *is* engaging in a certain task can override the indirect information from \mathbf{Y}_t and hence sharpen inference on state W_t . A simple measure of threat is given by the log odds score of each position at time t defined as $\rho_{it} = \log \frac{p(W_t=w_i|\mathbf{Z}_t)}{p(W_t=w_0|\mathbf{Z}_t)}$ for $i = 1 \dots 4$.

3 The criminal collaboration model

In the previous section, we reviewed the Bayesian hierarchical RVE model which can be used to model a suspected lone attacker’s progression to commit a certain crime. The focus in this paper is on modelling individuals who might be working in concert to commit a crime together. We describe our **criminal collaboration model** below.

3.1 The open population

Let Ω_t^* be the open population of Persons of Interest (POIs) at time t . Let $\Omega_t \subseteq \Omega_t^*$ be the subset of individuals that the authorities have decided to investigate and monitor at time t . For concreteness the size of Ω_t may be in the hundreds and Ω_t^* in the thousands (Doward, 2020; Sabbagh, 2020; Anderson, 2016). During each time period, new leads are discovered. New investigative cases are opened for those that pass a triage process meeting defined criteria⁴. The triage process thus gives rise to a set of newly identified individuals⁵ Ω_t^+ who join the set Ω_t . Over the same period, a set Ω_t^- are lost from Ω_t for a variety of reasons as discussed in Section 1. For simplicity, assume that Ω_t^+ join the set Ω_t at the start of the time period t and existing individuals Ω_t^- are lost at the end of t . Thus we have

$$\Omega_t = \{\Omega_{t-1} \setminus \Omega_{t-1}^-\} \cup \Omega_t^+.$$

We represent the *conspiratorial link* between individuals $\omega_i, \omega_j \in \Omega_t$ at time t by the random variable ϕ_{ijt} . Notice that this conspiratorial link is a latent variable and cannot be directly observed. We infer it from the observable behaviours, communications data and personal information of the individuals. Denote by Φ_t the symmetric *conspiracy matrix* at time t with elements ϕ_{ijt} . Here set $\phi_{iit} = 0$, for all $\omega_i \in \Omega_t$.

⁴These criteria include i) Risk: is there any evidence of risk in intelligible form, ii) Credibility: is the information reliable; iii) Actionable: can anything actually be done about it; iv) and Proportionality: is investigation of the lead necessary and proportionate within legal and statutory obligations, resources and priorities (London, 2019; BBC, 2019).

⁵This is a simplification as a subset of these individuals may already be known individuals in other contexts; moreover a lead may consist of information such as anonymous online posts that do not directly link to any known person. However ultimately any lead or case is aimed at discovering an individual or group of individuals that plan a crime and it is in this sense that we talk of “individuals” (London, 2019).

3.2 Prior knowledge and data

Collaboration between individuals gives rise to observable data of various kinds. It is generally difficult to unpick whether each observable action is criminal or benign. However, a collection of observations when used in conjunction with personal information on the individuals, can be indicative of the criminality of these behaviours and communications. There are at least six types of potentially knowable or observable data:

- Existing kinship or social links;
- Work or other shared affiliations;
- Bilateral electronic communications (telephone, email, Whatsapp etc);
- Broadcast electronic communications (e.g. conference versions of the above, facebook, twitter etc);
- Physical meetings (observed directly or through closed circuit television);
- Financial transactions (e.g. bank transfers between accounts).

The first two items are relatively static whereas the last four are more dynamic. Moreover the first two are not caused by criminal collaboration, but may enable a pre-existing tie that facilitates collaboration once other factors have come into play. Examples of these ties are the school and social ties that existed between several of the Al-Qaeda September 11, 2001 terrorists (Krebs, 2002), the kinship tie between Saleem and Hashem Abedi, the former being the suicide bomber of the May 22, 2017 Manchester Arena bombing (BBC, 2020), the latter his brother who was found guilty of aiding Saleem (Parveen and Walker, 2020), and the community ties surveyed by the US army in Thailand villages in 1965 (Meter, 2002).

Policing authorities typically receive information from multiple channels. Some example channels are the monitoring of physical meetings, interception of electronic communications, and intelligence obtained from other policing agencies, covert informants, or the public. Suppose that there are m such *information channels*. Denote by s_{ijkt} a summary measure of the information observed between individuals $\omega_i, \omega_j \in \Omega_t$ from channel k at time t . This summary measure can take a variety of forms depending on the type of information such as a sum of the observations (e.g. duration of phone calls) or a first-order difference (e.g. increase or decrease in money exchanged from one time to the next). Denote by U_t the *observations matrix* at time t with elements u_{ijt} such that $u_{ijt} = \{s_{ij1t}, \dots, s_{ijmt}\}$. Notice that U_t is also a symmetric matrix with $u_{ijt} = u_{jit}$. Note that we use the convention that u_{ijt} is an m -dimensional zero vector whenever $i = j$ and whenever no information is observed between two individuals. To indicate the difference in the quality of information obtained from the different channels, we define a parameter $\xi_k, k = 1, \dots, m$ which denotes the *relative efficiency* of the intelligence obtained from channel k .

Finally, we note that it is important to differentiate two types of data associated with communications: the content of such communications and “secondary

data”, i.e. metadata such as the identities of parties and the timing, location and duration of communications. Often secondary data is available whilst content data is unavailable due to either encryption or limits prescribed by certain interception warrants. Secondary data even without content data has proven to be extremely useful in tracing contacts, associations and habits (Anderson, 2016). Our model assumes at a minimum some availability of secondary data.

3.3 The network

Before we describe how the latent levels of collaboration given by conspiratorial links can be estimated, it is useful to construct a network of the individuals in Ω_t . The possible links between individuals can be described through an undirected weighted network \mathcal{N}_t at time t . Define the graph of \mathcal{N}_t as follows

$$\mathcal{N}_t = (V(\mathcal{N}_t), E(\mathcal{N}_t))$$

where $V(\mathcal{N}_t) = \Omega_t$ is the set of nodes and $E(\mathcal{N}_t)$ are the edges of the network. An edge exists between two individuals ω_i and ω_j if:

1. At some point in the past the pair enjoyed significant ties, such as being in the same extended family, being close friends, being arrested, stopped and searched, or imprisoned together.
2. *Since both becoming POIs* they have been observed communicating; such information may be gained through direct surveillance and monitoring, or intelligence gained through secondary sources.

These edges correspond to the pairs of individuals whose communications the authorities observe. Suppose that an edge exists between ω_i and ω_j . The weight on this edge will be given by the conspiratorial link ϕ_{ijt} contained in the symmetric conspiracy matrix Φ_t . Observe that unlike most weighted networks in the literature, the edge weights here are *distributions* instead of point estimates.

Example 1. *Three individuals $\omega_1, \omega_2, \omega_3$ have been seen to have posted pro-terrorist material on social media and have been triaged into Ω_t the observed population at time t : they are being investigated and their communications are being monitored. Further investigation reveals that ω_1 and ω_2 attended the same secondary school and are the same age, and that ω_2 and ω_3 attend the same gym and are frequently seen together. Due to these pre-existing links, the model forms edges between their representative nodes at time t , see Figure 3a. At time $t + 1$ a separate lead reveals the return of an individual ω_4 from Syria who was known to also have pro-terrorist ideas. It is suspected that he went to Syria for terrorist training. This information is represented in Figure 3b. At time $t + 2$ it is discovered that mobile phones newly registered to the addresses of ω_1 and ω_4 are in communication. This creates a tie between ω_1 and ω_4 as shown in Figure 3c and over the next few weeks the communications and activities of the four individuals are monitored.*

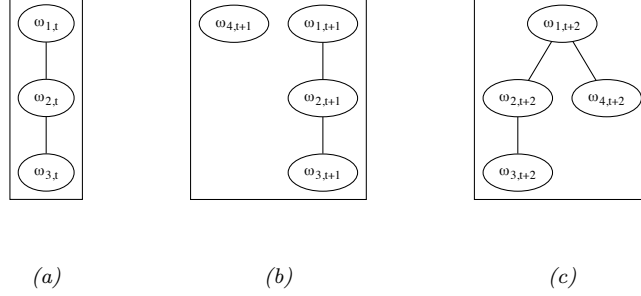


Figure 3: Structure of subnetwork at times t , $t+1$ and $t+2$

3.4 Setting up the model

Next we consider the task of estimating the weights on the edges of each network \mathcal{N}_t , $t \geq 0$. The latent levels of collaboration specified by Φ_t are estimated using the observable data in U_t . Let \mathcal{F}_t^- denote all the past information *up to time t* . \mathcal{F}_t^- includes $\{\mathcal{P}_{\Phi_s}\}_{0 \leq s < t}$ and $\{U_s\}_{0 \leq s < t}$, where \mathcal{P}_{Φ_s} is the distribution of Φ_s . With the help of the following simplifying assumptions, Φ_t can be easily estimated from U_t and Φ_{t-1} for each time t using the steady model described in Section 3.5; thus allowing for fast real-time updates. Here $\perp\!\!\!\perp$ indicates probabilistic independence.

- **Assumption 1:** (Pairwise link independence) The conspiratorial links for each pair $\{w_i, w_j\}$ are mutually independent at time t given the past.

$$\perp\!\!\!\perp_{\{w_i, w_j\} \in \Omega_t \times \Omega_t} \phi_{ijt} \mid \mathcal{F}_t^-.$$

- **Assumption 2:** (First-order Markov property) $\phi_{ijt} \in \Phi_t$ is linked to the past only through $\phi_{ij,t-1} \in \Phi_{t-1}$.

$$\phi_{ijt} \perp\!\!\!\perp \mathcal{F}_t^- \mid \phi_{ij,t-1}.$$

- **Assumption 3:** (Output independence) The observations u_{ijt} for a pair $\{\omega_i, \omega_j\}$ at time t are only dependent on the latent conspiratorial link between them ϕ_{ijt} .

$$u_{ijt} \perp\!\!\!\perp (\Phi_t, U_t, \mathcal{F}_t^-) \mid \phi_{ijt}.$$

- **Assumption 4:** (Information independence) The intelligence from the various information channels for a $\{\omega_i, \omega_j\}$ at time t are mutually independent.

$$\perp\!\!\!\perp_{k \in \{1, \dots, m\}} s_{ijk t}$$

Although some of these assumptions may not hold in reality they are useful for our initial model and the necessity for relaxation will be evaluated as work

progresses. For any application using our model, statistical diagnostics must always be run to measure the extent of the validity of these assumptions. This is, however, beyond the scope of this paper and henceforth we take these assumptions to be valid. The relationship between the observation and conspiracy matrices can then be represented as a two time-slice dynamic Bayesian network (2TS-DBN) whose graph is shown in Figure 4.



Figure 4: Graphical representation of the 2TS-DBN: (a) on a univariate level; (b) on a multivariate level (labelled as graph \mathcal{G}).

Theorem 1. *Under the assumptions described above, the marginal likelihood of the 2TS-DBN represented by the graph \mathcal{G} decomposes into the product of the one step ahead forecasts. Additionally all elements of U_t and Φ_t can be updated independently.*

The proof can be found in Appendix A of the supplementary materials.

3.5 The steady model

Under non-Gaussian settings the derived one step ahead recurrences needed to update distributions of Φ_t in our network are often not in closed form. In such cases sampling or approximation would be required. Although sequential approximations such as those used in variational inference have some attraction, in our context, approximate methods would generally be prohibitive in terms of the computational demand. However, by an appropriate choice of the state space representation we can retrieve exact formulae for the one step ahead predictive distributions.

In this paper, we adopt the approach of using a *steady model* from Gaussian dynamic linear models (West and Harrison, 1997). In a general sense, the steady model manipulates the posterior at time $t - 1$ into a prior for time t such that the mean is kept steady with a more diffuse variance. Here, we adapt the steady model into a non-Gaussian conjugate Gamma-Poisson setting (Smith, 1979, 1981; Smith and Freeman, 2010). Interestingly, a different non-Gaussian variation of this model has also been applied to modelling online traffic flow count data in (Chen et al., 2018). Below we outline our Gamma-Poisson steady model to estimate Φ_t .

From the setup of the multivariate 2TS-DBN in Section 3.4, we can model the conspiratorial link ϕ_{ijt} using observational data u_{ijt} for each pair $\{\omega_i, \omega_j\}$ independently.

Initialisation: For each pair $\{\omega_i, \omega_j\}$, set the prior ϕ_{ij,t_0} as follows

$$\phi_{ij,t_0} \sim \text{Gamma}(\alpha_{ij,t_0}, \beta_{ij,t_0}) \quad (3)$$

where t_0 is the first time period in our time-series. The parameters α_{ij,t_0} and β_{ij,t_0} are determined by existing case knowledge. For example, if $e(\omega_i, \omega_j) \in E(\mathcal{N}_{t_0})$ exists only due to a social relation α_{ij,t_0} and β_{ij,t_0} may be set such that the mean and variance of ϕ_{ij,t_0} are both relatively low. Whereas if ω_i and ω_j have a previous joint conviction then these parameters can be set such that the ϕ_{ij,t_0} has a high mean and lower variance.

Posterior at time $t-1$: Let the posterior of $\phi_{ij,t-1}$ after observing $u_{ij,t-1}$ and \mathcal{F}_{t-1-} be given by

$$\phi_{ij,t-1}|u_{ij,t-1}, \mathcal{F}_{t-1-} \sim \text{Gamma}(\alpha_{ij,t-1}, \beta_{ij,t-1}) \quad (4)$$

Prior at time t : Under the steady model, we use a discount factor $\delta_{ijt} \in (0, 1)$ to evolve the posterior at time $t-1$ to the prior at time t as follows.

$$\phi_{ijt}|\mathcal{F}_{t-} \sim \text{Gamma}(\delta_{ijt}\alpha_{ij,t-1}, \delta_{ijt}\beta_{ij,t-1}). \quad (5)$$

The discount factor δ_{ijt} represents the decay of information from time $t-1$ to time t . Scaling the parameters by δ_{ijt} gives us the steady evolution in our model.

Information generation at time t : Recall that from the information independence assumption in Section 3.4, the observations from the different information channels can be modelled independently. We assume that the observations from the information channels are generating through the following distribution

$$s_{ijkt}|\phi_{ijt}, \mathcal{F}_{t-} \sim \text{Poisson}(\xi_k \phi_{ijt}), \quad k = 1, \dots, m. \quad (6)$$

Posterior at time t : Then the posterior when the observation vector u_{ijt} has at least one non-zero element is given by

$$\begin{aligned} p(\phi_{ijt}|u_{ijt}, \mathcal{F}_{t-}) &\propto \prod_{k=1}^m p(s_{ijkt}|\phi_{ijt}, \mathcal{F}_{t-}) p(\phi_{ijt}|\mathcal{F}_{t-}) \\ \phi_{ijt}|u_{ijt}, \mathcal{F}_{t-} &\sim \text{Gamma}(\alpha_{ijt}, \beta_{ijt}) \end{aligned} \quad (7)$$

where $\alpha_{ijt} = \delta_{ijt}\alpha_{ij,t-1} + \sum_k s_{ijkt}$ and $\beta_{ijt} = \delta_{ijt}\beta_{ij,t-1} + \sum_k \xi_k$.

One step ahead forecast: The one step ahead forecast of the information from channel k can be obtained in closed form as

$$\begin{aligned} p(s_{ijk,t+1}|\mathcal{F}_{t+1-}) &= \int_{\phi_{ij,t+1}} p(s_{ijk,t+1}|\phi_{ij,t+1}, \mathcal{F}_{t+1-}) p(\phi_{ij,t+1}|\mathcal{F}_{t+1-}) d\phi_{ij,t+1} \\ &= \binom{s_{ijk,t+1} + \delta_{ij,t+1}\alpha_{ijt} - 1}{s_{ijk,t+1}} \frac{(\delta_{ij,t+1}\beta_{ijt})^{\delta_{ij,t+1}\alpha_{ijt}} \xi_k^{s_{ijk,t+1}}}{(\xi_k + \delta_{ij,t+1}\beta_{ijt})^{(\delta_{ij,t+1}\alpha_{ijt} + s_{ijk,t+1})}}. \end{aligned} \quad (8)$$

In settings such as ours, it is essential to differentiate between the following cases:

1. $\sum_k s_{ijkt} = 0$ because ω_i and ω_j were monitored but did not communicate in any way during time t ;
2. $\sum_k s_{ijkt} = 0$ because ω_i and ω_j were not closely monitored during time t .

In the first case, the posterior update is carried out as described above. In the second case, the prior at time t is set as the posterior at time t , i.e. a posterior update using the data is not carried out. This ensures that when we haven't actually *observed* zero communications, the posterior mean at time t is the same as the posterior mean at time $t - 1$ and the posterior variance increases from time $t - 1$ to t .

The distribution of the latent level of collaboration can hence be periodically updated in closed form using the above recurrences across the network given the sequential incoming observational data. Also, the dynamic nature of the open population is easily incorporated in our model by introducing vertices, edges and priors for immigrants (new entrants) and removing them for emigrants (leavers) at the appropriate time.

4 Integrating system and cell-level threat measure

Having presented the criminal collaboration model we now integrate this with the individual RVE models (see Section 2). The RVE model is used for individuals belonging to Ω_t at time t . This combination forms the basis of an *integrated decision support system* (IDSS) for the counter-terrorism authorities. We then show that estimation and inference for the criminal collaboration model and the individual RVEs can be performed independently even under the IDSS by assuming certain conditional independences across the process. Finally, we utilise the independent estimation of parameters across the IDSS to arrive at a measure of imminence of threat posed by a known or suspected group of collaborating individuals within Ω_t .

It is appropriate here to technically define what we mean by a *cell* in this model. We define here a cell C as a possibly strict subset of a connected component X of the collaboration network $C \subseteq X \subseteq \mathcal{N}_t$ that the investigators, *based on their expert judgement*, determine to be an *organisational unit for potential attack*. Recall that the network connections are formed either by existing ties known by the investigators or observed communications post entry into Ω . More sophisticated methods for identifying clusters exist in network theory and there are various definitions of what constitutes a terrorist cell in terrorism research (Shapiro, 2005). However for our purposes we take this simple definition. More nuanced definitions of cells, and more sophisticated methods of identifying them will be addressed in future work.

4.1 Integrated decision support system

The success of any attempts to carry out a group attack is not only informed by the latent levels of collaboration between pairs of individuals within a criminal cell but also by the threat posed by each member of such a cell. Thus in order to analyse any network of criminal collaborations among a population Ω_t of suspected criminals, the model must also be linked to the individual RVEs of each member $\omega \in \Omega_t$.

Define the following

$$\begin{aligned}\Theta_t &= \{\theta_{\omega t} : \omega \in \Omega_t\} \\ \mathbf{Z}_t &= \{\mathbf{Z}_{\omega t} : \omega \in \Omega_t\} \\ \mathbf{W}_t &= \{W_{\omega t} : \omega \in \Omega_t\}\end{aligned}$$

where $\theta_{\omega t}$, $\mathbf{Z}_{\omega t}$ and $W_{\omega t}$ are defined as in Section 2 for the RVE of $\omega \in \Omega_t$.

The communications observed between a pair $\{\omega_i, \omega_j\}$ given by u_{ijt} is closely linked to the data on these individuals given by $\mathbf{Y}_{\omega_i t}$ and $\mathbf{Y}_{\omega_j t}$. This relates u_{ijt} to the task intensities $\mathbf{Z}_{\omega_i t}$ and $\mathbf{Z}_{\omega_j t}$ for ω_i and ω_j 's individual RVEs respectively. Thus from the observation matrix U_t , we can construct a vector $\mathbf{u}_t = \{u_{\omega t} : \omega \in \Omega_t\}$ where $u_{\omega t}$ is a function of U_t reflecting the totality of information exchanges between ω and those they⁶ are in contact with. Using this link, we can combine the two types of models into an integrated decision support system (Leonelli and Smith, 2015). We first set out the assumptions where \mathcal{F}_{t-}^* is all the past information up to time t contained in the individual RVEs and the criminal collaboration model.

- **Assumption 1:** (Mutual independence given task intensity) The individual RVE models are mutually independent given task intensities.

$$(W_{\omega_i t}, \theta_{\omega_i t}) \perp\!\!\!\perp (W_{\omega_j t}, \theta_{\omega_j t}) | \mathbf{Z}_t$$

- **Assumption 2:** (Initial prior threat independence) The prior parameters of the RVE models and the collaboration model are independent

$$(W_0, \Theta_0) \perp\!\!\!\perp \Phi_0.$$

- **Assumption 3:** (Threat states are Markov) The threat states are linked to the past \mathcal{F}_{t-}^* only through the latest threat states.

$$(W_t, \Theta_t) \perp\!\!\!\perp \mathcal{F}_{t-}^* | (W_{t-1}, \Theta_{t-1}).$$

- **Assumption 4:** (Conditional instantaneous independence) The current task intensities are independent of the past given the current task set and the current total communications of each individual.

$$\mathbf{Z}_t \perp\!\!\!\perp \mathcal{F}_{t-}^* | \Theta_t, \mathbf{u}_t.$$

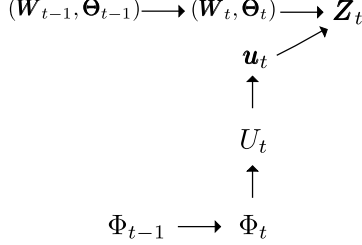


Figure 5: Graph of the IDSS.

With these assumptions, the IDSS can be represented by the graph in Figure 5.

Theorem 2. *The collaboration model and the individual RVEs in the IDSS model developed under the above assumptions can be decoupled.*

See the proof using the d-separation theorem in Appendix B of the supplementary material.

4.2 Cell-level threat measure

Here we demonstrate how through a simple yet effective combination of factors we can quantify the imminence of the threat posed by cells. The threat measure can be plotted against time to analyse how the threat posed by the cell develops dynamically. Theorem 2 enables us to combine the outputs from the criminal collaboration model (Section 3) with the individual RVE models (Section 2) to arrive at a holistic threat measure.

The resources available to the authorities are limited and so it is critical that they are able to identify which cell poses the most imminent threat. To enable quick real-time support, we need a measure that can be readily calculated from the available information and easily interpreted by the authorities. As a basic requirement, we need that the subgraph of \mathcal{N}_t induced by the members of a suspected cell C is connected. To carry out a collaborative attack, each individual in C needs to be in contact with at least one other individual in C , otherwise a joint effort would not be possible. We now present a threat measure for a suspected terrorist cell C considering the following factors described below.

(1) Collective progress: The development of the plot being pursued collectively by the cell can be indicated by a latent threat state $W_t^C \in \{w_0^C, \dots, w_k^C\}$. Similar to Section 2, the available data \mathbf{Y}_t^C can be used to inform the status of completion of a set of hidden tasks $\boldsymbol{\theta}_t^C$ associated with the plot through a signal of task intensities \mathbf{Z}_t^C . A probability vector $\boldsymbol{\pi}_t^C = \{\pi_{1t}^C, \dots, \pi_{kt}^C\}$, indicating the probability of being in the k threat states at time t , can be obtained through

⁶We use “they” and “their” as indefinite gender singular pronouns

the recurrence in Equations 1-2. However, in such a collaborative unit, there will be some tasks that need only be done by a subset of members of the cell; for example figuring out the logistics or developing certain skills. Thus, the signal \mathbf{Z}_t^C obtained from the collective data on the cell \mathbf{Y}_t^C must be set against these requirements to indicate whether the tasks are being sufficiently completed. Let $\mathbf{T}^C \subset W_t^C$ indicate the set of threat states considered to be most dangerous by the authorities. As an example we can set $\mathbf{T}^C = \{\text{Preparing}, \text{Mobilised}\}$. A measure of *preparedness* of the cell can be obtained as

$$m_1 = \sum_{w_i^C \in \mathbf{T}^C} \pi_{it}. \quad (9)$$

(2) Individual threat: Recall that the individual RVE represents the progress made by an individual on a plot they plan to enact themselves. By considering the the same plot being pursued by the cell for the individual RVEs of the members, we are likely to underestimate the threat of each member. This happens as the cell needs to collectively have the capability to enact the plot and each individual need not be part of every task associated with the plot. Ideally we would be able to identify with each member of C the role that they play within the cell. Each role can then have an associated set of tasks. However, this is not always possible as it requires detailed understanding of the cell's dynamics.

One option is to evaluate the threat status of the individuals in C based on their progress on the tasks $\theta_t^* \subset \theta_t^C$ that most of the members of C are expected to have the skills to do. The threat states for the individual RVEs can be adapted in line with this to obtain the sum of measures of *individual threat* for each member of C as

$$m_2 = \prod_{\omega \in C} \left\{ \sum_{w_i \in \mathbf{T}} \pi_{it}^\omega \right\} \quad (10)$$

where \mathbf{T} denotes the set of most dangerous threat states in the individual RVEs.

(3) Latent collaboration: In any cell, we may not expect each pair to be communicating with each other but for any successful collaborative project, a certain amount of connectivity is expected between each communicating pair and overall in the cell. Hence we set up two different measures of *cohesion*. For each communicating pair $\{\omega_i, \omega_j\}$ in C , we measure pairwise cohesion as

$$m_3^* = p(\phi_{ijt} > x_1) \quad (11)$$

where x_1 is the lower limit of how much we expect each pair to be communicating for the plot to be enacted. A cell-wide measure of pairwise cohesion can be obtained as

$$m_3 = \prod_{\{\omega_i, \omega_j\} \in \Omega_t \times \Omega_t} p(\phi_{ijt} > x_1). \quad (12)$$

Similarly, a cell-level cohesion measure can be obtained from the subnetwork *density* of C

$$m_4 = \frac{k}{\binom{n}{2}} \quad (13)$$

where $k = |E(C_t)|$ is the number of ties of the subnetwork representing the cell $C \in \mathcal{N}_t$ at time t , $n = |C_t|$ is the size of the cell C and thus $\binom{n}{2}$ is the number of possible ties in C .

(4) Size of the cell: While collaborative efforts benefit from sharing resources and skills, a very large cell can be unwieldy and increases the risk of exposure of the cell. For a given plot, the authorities are likely to be able to estimate an ideal cell size n^* . A simple measure of *cell integrity* is obtained as

$$m_5 = \text{sech}\left(\frac{n - n^*}{n^*}\right) \quad (14)$$

Cell threat score: For a given plot, a cell is most threatening when $m_1 = m_2 = m_3 = m_4 = m_5 = 1$. We can obtain an ordered set of cell based threat scores $\{\varphi_C(i)\}$, $i \in \{0, \dots, 4\}$ as

$$\varphi_C(i) = \prod_{j=1}^{5-i} m'_j \quad (15)$$

$$\{m'_j\}_{j=1, \dots, 5} = \sigma(\{m_i\}_{i=1, \dots, 5})$$

where σ is a reordering of elements from high to low so that for $i = 1 \dots 4$

$$0 \leq m'_{i+1} \leq m'_i \leq 1$$

and hence for $i = 0 \dots 3$

$$0 \leq \varphi_C(i) \leq \varphi_C(i+1) \leq 1$$

This ordered set is used to check whether a single or few measures' values are overly affecting the base $\varphi_C(0)$ score. Each of these scores has the property that a higher value of $\varphi_C(i)$ indicates a greater imminence and danger of the threat posed by the cell C . Thus we have combined several key factors to obtain a transparent threat score for a cell which can guide the authorities to prioritise and de-prioritise cases. Note that this score can be easily adapted to incorporate other elements that may be considered to be essential by the policing authorities.

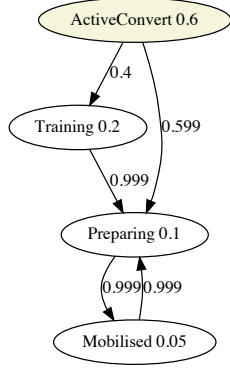
5 Simulation

In this penultimate section we develop Example 1 from Section 3.3 with a synthetic data scenario. The actual observational and communications data available to the policing authorities are classified. The synthetic data we use is

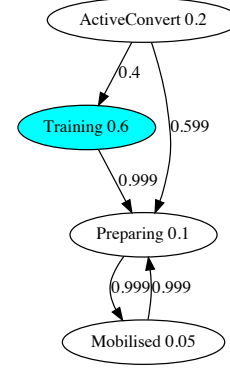
based on meetings with authorities and public source data on a variety of actual cases. We illustrate the dynamics of the collaboration model, the extension of the individual RVE model to a cell based RVE model, and the coupling of the criminal collaboration model with the RVE model to produce cell level threat measures. We keep the network small both as this is realistic to several terrorist incidents and in order to maintain clarity of exposition. Since the model equations throughout are in closed form the model scales to larger networks.

5.1 Scenario

Recall from example 1 that three individuals ω_1, ω_2 , and ω_3 have been triaged into Ω_t based on their pro-terrorist social media posting and a fourth ω_4 based on their suspected terrorist training in Syria. They are all known to live in the North East area of the same city. Ties between the first three have been created due to existing school and gym affiliations, and a tie between ω_4 and ω_1 has been created based on mobile phone communication. Based on this information prior probabilities of their *individual* threat positions in the RVE model are set as depicted in Figure 6. Since ω_4 is known to have returned from Syria and believed to have trained there, their probability of being in the **Training** position is high; whilst for the others their stated views indicates high probability of being in the **ActiveConvert** position.



(a) RDCEG for $\omega_1, \omega_2, \omega_3$; node labels are prior position probabilities; edge labels are position transition probabilities i.e. elements $m_{i,j}$ of matrix M^0 in Table 1.



(b) RDCEG for ω_4 : Note due to prior information the probability of ω_4 being in training is higher than for the other individuals.

Figure 6: Reduced Dynamic Chain Event Graph for individuals with prior position and edge probabilities

As these four individuals are in the set Ω_t their activities and communica-

tions are being monitored. Over the next weeks ω_1 's internet activity includes repeated visits to car dealer and car rental websites, and to knife retailers. Data from their bank account shows a large increase in funds from an overseas bank transfer. ω_2 's internet activity includes visits to illegal bomb making websites and to extremist radical websites. ω_4 's internet activity includes online map searches of government buildings and densely populated commercial areas of the city. They physically visit potential bomb testing sites. The observed activity data for each individual are shown in Figure 7. This data is used in the RVE model.

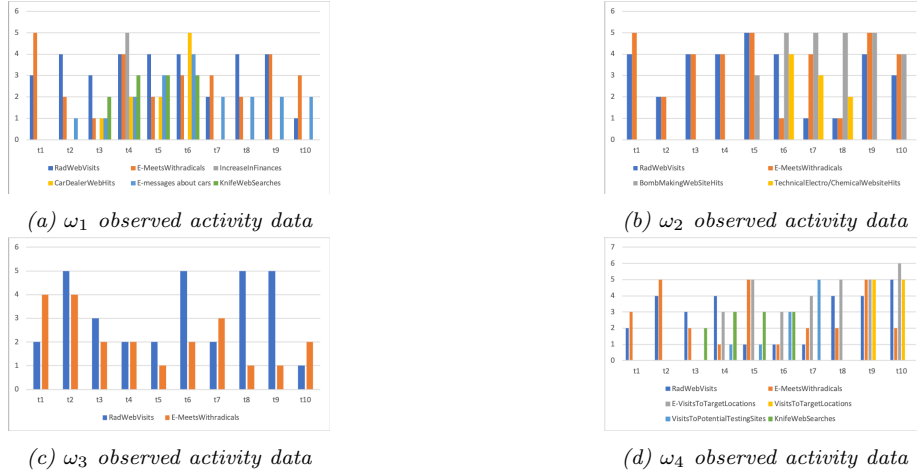


Figure 7: Activity data for the individuals in the cell over the observed time period

We move on to the communications data for the collaboration model which is observed over the same time period as the activity data. For simplicity in this example we suppose observations of the communications between these individuals comes from a single channel: mobile phone calls. Table 2 shows the sum of the calls in hours observed between each pair over a period of ten weeks t_1 to t_{10} . Figure 8 charts this data. From week 2 to week 4 the pair (ω_1, ω_2) who attended the same secondary school talk over their mobile phones at a consistent rate. In week 3 ω_1 calls ω_4 the returnee from Syria. In week 5 ω_1 converses with ω_3 and ω_2 converses with ω_4 . These new calls create new ties in the network. By week 6 all four individuals are mutually communicating⁷ and the total times of these calls increase from weeks 7 to 10.

5.2 Collaboration model application

Using the Gamma-Poisson steady model described in Section 3.5, we specify the prior distribution of latent criminal collaboration by means of setting the α and β parameters for each pair with known ties. As discussed this is based on

⁷Thus technically the subgraph of the cell is now a *complete graph*.

any information known at that time about the pair. The communications data then updates the posterior for each pairs' latent criminal collaboration at each week.

| | $s_{1,2}$ | $s_{1,3}$ | $s_{1,4}$ | $s_{2,3}$ | $s_{2,4}$ | $s_{3,4}$ |
|-----|-----------|-----------|-----------|-----------|-----------|-----------|
| t1 | 0 | 0 | 0 | 0 | 0 | 0 |
| t2 | 3 | 0 | 0 | 1 | 0 | 0 |
| t3 | 5 | 0 | 2 | 0 | 0 | 0 |
| t4 | 5 | 0 | 5 | 0 | 0 | 0 |
| t5 | 5 | 5 | 5 | 0 | 2 | 0 |
| t6 | 5 | 6 | 6 | 5 | 6 | 5 |
| t7 | 7 | 6 | 7 | 6 | 7 | 7 |
| t8 | 6 | 6 | 8 | 4 | 8 | 8 |
| t9 | 7 | 7 | 9 | 7 | 9 | 9 |
| t10 | 7 | 8 | 11 | 8 | 10 | 10 |

Table 2: Simulated weekly mobile phone call data of pairs of individuals in collaboration network

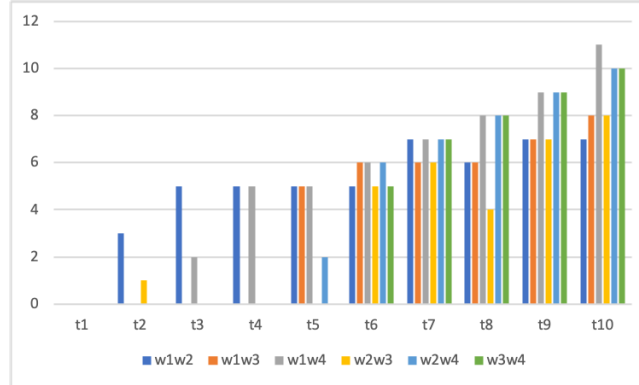
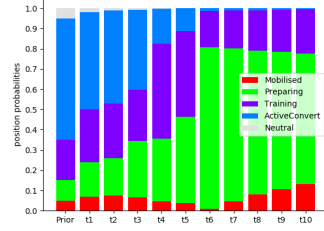
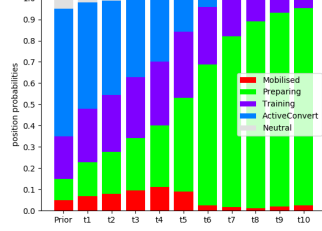


Figure 8: Histogram of mobile phone data

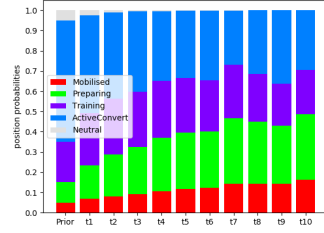
The resulting α and β parameters from the Gamma-Poisson steady network model are shown in Table 5 and the means and standard deviations are shown in Table 6 both in Appendix C of the supplementary material Bunnin et al. (2020). The evolution of the latent collaboration distributions through time are shown in Figure 11 and the evolution of the individual threat position probabilities are shown in Figures 9. The final posterior position probabilities at time t_{10} for each individual's RDCEG from the RVE model are shown in Figure 10.



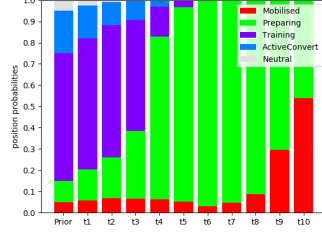
(a) Position probabilities through time for ω_1



(b) Position probabilities through time for ω_2

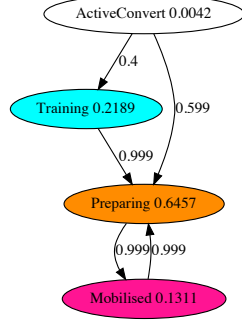


(c) Position probabilities through time for ω_3

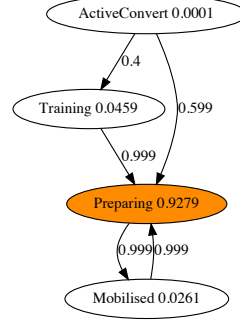


(d) Position probabilities through time for ω_4

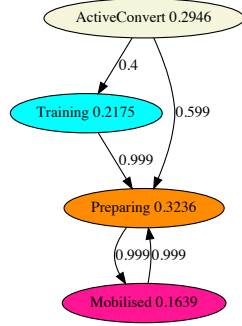
Figure 9: Posterior probabilities through time from the RVE model for individuals



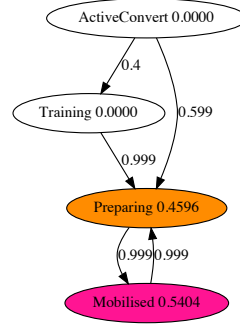
(a) RDCEG for ω_1



(b) RDCEG for ω_2

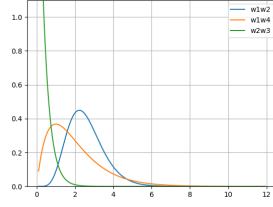


(c) RDCEG for ω_3

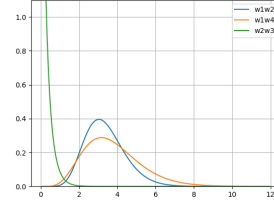


(d) RDCEG for ω_4

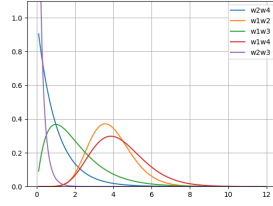
Figure 10: Posterior probabilities from the RVE model for individuals



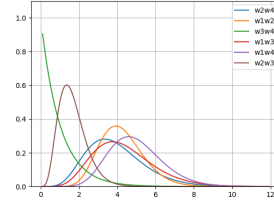
(a) posterior density at t_3



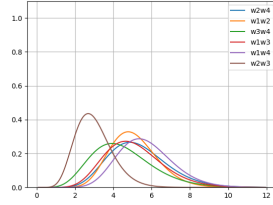
(b) posterior density at t_4



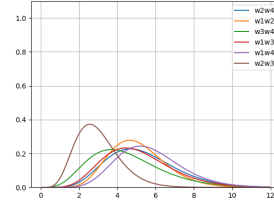
(c) posterior density at t_5



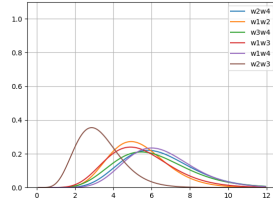
(d) posterior density at t_6



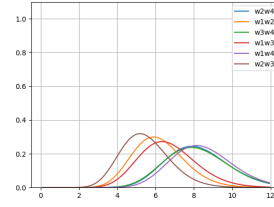
(e) posterior density at t_7



(f) posterior density at t_8



(g) posterior density at t_9



(h) posterior density at t_{10}

Figure 11: Latent level of criminal collaboration between pairs of individuals in the network inferred as evolving densities ϕ_t using the Gamma-Poisson steady model

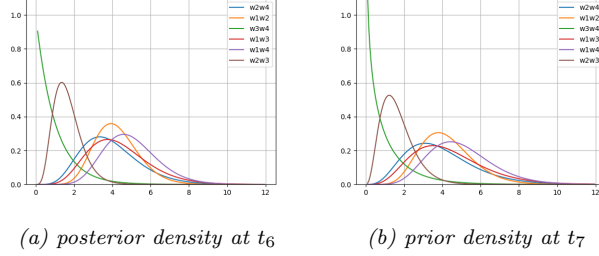


Figure 12: Illustration of increased dispersion for ϕ densities from t_6 posterior to t_7 prior using the Gamma-Poisson steady model. The means and standard deviations of the prior densities (see Table 6) set at the first time a tie is modelled reflects what the authorities know about their level of collaboration and the uncertainty associated with it. To obtain the prior for week t_{n+1} , the discount factor is applied to the parameters of the posterior at time t_n . From the prior densities shown in this figure and from Table 5, we can see that the variance of the priors for t_{n+1} increases compared to the variance of the posteriors for the week before that (t_n), while the means are kept stable. This reflects that at the start of every new week, before any new data is processed, we expect the level of collaboration between each pair to have remained the same as it was last week but we are less sure of this now.

As the total times of the calls increase the collaboration densities move to the right (see Figure 11). This indicates higher probabilities of collaboration towards an attack. The individual RVE models results (see Figure 9) are consistent with these results. In the next section we illustrate the results from the coupling of the RVE and collaboration models.

5.3 Cell level RVE model and threat score

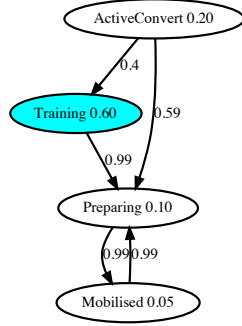
As discussed in Section 4.2 we construct a cell based RVE model with the combined task sets and combined observational data on the individuals believed to be part of the cell. We take the position probabilities of the individual within the cell with highest prior threat, ω_4 , as the prior probabilities for the cell level RDCEG. We then calculate joint task intensities based on the data from *all* the individuals in the network. From the task intensities the cell position probabilities are propagated as in the individual RVE model; i.e. using Equations 1 and 2. The prior and posterior network and RDCEG for the cell is shown in Figure 13 and the evolution through time in Figure 14. As can be seen the threat state probability for the position **Preparing** increases from week 5 as activity and communications increase, and in weeks 9 and 10 the probability for the cell to in position **Mobilised** sharply increases. The numeric cell threat measures m_1 to m_5 and the combined scores φ_C are shown in Table 3. If we signal a warning when φ_C reaches a certain threshold, say 0.15 then we can see that for $\varphi_C(0)$ this is not reached till time t_7 whereas for $\varphi_C(2)$ this is reached by time t_3 . In practise we would expect the investigators to calibrate such measures and thresholds using experience and judgement, and thus this is work in progress.

To summarise, this worked example demonstrates how observed activity data and communications data combined with prior distributions calibrated to

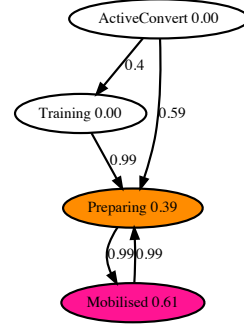
investigator’s knowledge can give real-time measures of dynamic threat at the cell and individual levels. The strengths of latent criminal collaboration and the latent threat state probabilities are estimated dynamically based on the incoming data.

In this particular scenario, with synthetic data informed by real cases, the results show a marked increase in threat levels driven by the increase in specific activity data and mobile phone call times. This is shown in by large increases in the **Preparing** probability for the cell at times t_5 and t_6 and then increases at times t_9 and t_{10} for the **Mobilised** probability. In terms of cell threat score this is reflected in the increase in $\varphi_C(2)$ from 0.27 at time t_4 to 0.57 at time t_6 and then reaching 0.88/0.89 for time t_7 to t_{10} .

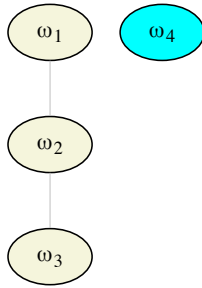
We have thus demonstrated how the collaboration model works using synthetic data and how it is coupled with the RVE model to produce cell level threat state probabilities and scores. The concluding section reviews the research and discusses future work.



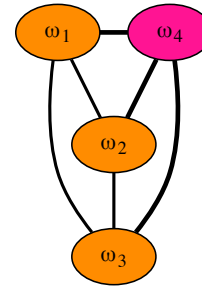
(a) RDCEG for cell with prior position probabilities



(b) RDCEG for cell with time t_{10} posterior position probabilities



(c) Collaboration network at time t_1 . Node colour indicates individual's position of highest probability.



(d) Collaboration network at time t_{10} . Edge width and colour indicates strength of tie.

Figure 13: Graphical depictions of the prior and posterior threat status of the terrorist cell using the integrated RVE and criminal collaboration models

| | Prior | t1 | t2 | t3 | t4 | t5 | t6 | t7 | t8 | t9 | t10 |
|----------------|-------|------|------|------|------|------|------|------|------|------|------|
| m1 | 0.15 | 0.21 | 0.26 | 0.32 | 0.45 | 0.71 | 0.96 | 0.99 | 1.00 | 1.00 | 1.00 |
| m2 | 0.00 | 0.00 | 0.01 | 0.01 | 0.04 | 0.09 | 0.22 | 0.31 | 0.32 | 0.31 | 0.36 |
| m3 | 0.14 | 0.05 | 0.14 | 0.04 | 0.03 | 0.00 | 0.30 | 1.00 | 1.00 | 1.00 | 1.00 |
| m4 | 0.67 | 0.67 | 0.67 | 0.67 | 0.67 | 0.67 | 0.67 | 0.67 | 0.67 | 0.67 | 0.67 |
| m5 | 0.83 | 0.83 | 0.83 | 0.89 | 0.89 | 0.89 | 0.89 | 0.89 | 0.89 | 0.89 | 0.89 |
| $\varphi_C(0)$ | 0.00 | 0.00 | 0.00 | 0.00 | 0.00 | 0.00 | 0.04 | 0.18 | 0.19 | 0.19 | 0.21 |
| $\varphi_C(1)$ | 0.01 | 0.01 | 0.02 | 0.01 | 0.01 | 0.04 | 0.17 | 0.58 | 0.59 | 0.59 | 0.59 |
| $\varphi_C(2)$ | 0.08 | 0.12 | 0.14 | 0.19 | 0.27 | 0.42 | 0.57 | 0.88 | 0.88 | 0.89 | 0.89 |
| $\varphi_C(3)$ | 0.55 | 0.55 | 0.55 | 0.59 | 0.59 | 0.63 | 0.86 | 0.99 | 1.00 | 1.00 | 1.00 |
| $\varphi_C(4)$ | 0.83 | 0.83 | 0.83 | 0.89 | 0.89 | 0.89 | 0.96 | 1.00 | 1.00 | 1.00 | 1.00 |

Table 3: Cell level measures of threat resulting from integration of RVE and collaboration models. m_1 to m_5 give individual measures of aspects of cell preparedness and cohesion. The various $\varphi_C(j)$ combine the m_i measures to give an overall score of cell threat. The argument to φ_C is the number of measures m_i omitted from the product, in order of smallest to largest i.e. $\varphi_C(1)$ omits $\min\{m_i\}_{i=1..5}$.

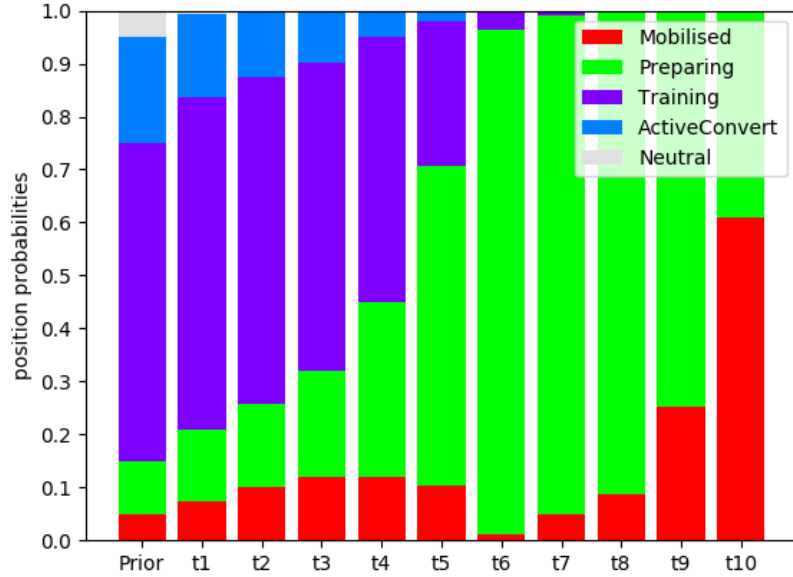


Figure 14: Visual display of cell level RVE model position probabilities through time based on combined individual activity data and assuming a joint task set shared between cell members.

6 Discussion

In this paper we have demonstrated how using various types of noisy and sparse data to which authorities typically have access, a criminal collaboration model can be developed to track, analyse and predict the collective activities of individuals acting in concert. We showed how this model can be combined with the individual RVE models presented in Bunnin and Smith (2019) to create an integrated decision support system. This support system produced both individual level and cell based measures of dynamic progress towards attack. The methods used in this paper are novel to this application and provide a way of setting the literature on social network models applied to this domain within a more flexible and statistically defensible framework for further exploration.

Within this domain uncertainty and hidden or false signals are key challenges. We have attempted to build our model in such a way that combinations of weak signals can be extracted and utilised given the preexisting knowledge of the investigators. Moreover the model can be modified or overridden at any point by manually changing parameters or creating or deleting ties as the investigators see fit. The working of the model are transparent relying purely on Bayesian updating and prior distribution inputs. Thus all results can be traced back to the data and the quantitative assumptions.

Going forward, there are several ways in which our models can be refined and extended. Preliminary explorations show that conventional clustering methods appear to have unsatisfactory performance in identifying potential cells directly from the dynamic network data. Moreover the noted characteristics of incompleteness and fuzzy boundaries need to be addressed in any algorithmic or statistical attempts to identify cell members.

Future work includes constructing methods to infer non-observed individuals from observational data and from domain knowledge on the organisational structure of cells. We are now starting to develop various stochastic set functions which can be used within a bespoke clustering framework for applications similar to our own. The early results of this work are promising and will be reported as a follow up to this paper. Also, while it would be of great practical importance to effectively identify weak ties as described by Sparrow (1991), it is difficult to distinguish these from benign low levels of communication and contact. Incorporating this with consideration of the dynamic network data $\{\mathcal{N}_s\}_{s \leq t}$ would be a useful line of future work.

Finally the generic architecture we construct might be applicable in other domains where there is a requirement to integrate individual time series with dynamic interactions where the individuals have a collaborative objective. Example are other social processes such as the development of different political pressure groups. In summary we provide a novel example of how to set about building a integrated decision support systems where the modelled social process involves complex interacting agents with shared goals.

References

- Allen, G. and Dempsey, N. (2018). Terrorism in great britain: the statistics. briefing paper number cbp7613. Technical report, House of Commons.
- Anderson, D. (2016). Report of the bulk powers review, presented to parliament. *Houses of Parliament*.
- BBC (2019). Analysis: Understanding the risks of terrorism. *Radio 4*.
- BBC (2020). Manchester arena attack: Brother’s fingerprints linked to arena bomb. *BBC*.
- Berlusconi, G., Calderoni, F., Parolini, N., Verani, M., and Piccardi, C. (2016). Link prediction in criminal networks: A tool for criminal intelligence analysis. *PloS one*, 11(4).
- Broccatelli, C., Everett, M., and Koskinen, J. (2016). Temporal dynamics in covert networks. *Methodological Innovations*, 9:2059799115622766.
- Bunnin, F. O., A.Shenvi, and Smith, J. Q. (2020). Supplementary material for network modelling of criminal collaborations with dynamic bayesian steady evolutions. *Bayesian Anal.*
- Bunnin, F. O. and Smith, J. Q. (2019). A bayesian hierarchical model for criminal investigations. *Bayesian Anal.* Advance publication.
- Campedelli, G. M., Cruickshank, I., and Carley, K. (2019). A complex networks approach to find latent clusters of terrorist groups. *Applied Network Science*.
- Chen, X., Irie, K., Banks, D., Haslinger, R., Thomas, J., and West, M. (2018). Scalable bayesian modeling, monitoring and analysis of dynamic network flow data. *Journal of the American Statistical Association*, 113.
- Cowell, R., Dawid, A., Lauritzen, S., and Spiegelhalter, D. (2001). *Probabilistic Networks and Expert Systems*, volume 43. Springer.
- Cunningham, D., Everton, S. F., and Murphy, P. J. (2015). *Casting More Light on Dark Networks*, page 171185. Structural Analysis in the Social Sciences. Cambridge University Press.
- Doward, J. (2020). Junior police must make split second decisions on terrorists. *The Guardian Newspaper*.
- Europol (2018). Terrorism situation and trend report. Technical report, European Union Agency for Law Enforcement Cooperation.
- Helfstein, S. and Wright, D. (2011). Covert or convenient? evolution of terror attack networks. *Journal of Conflict Resolution*, 55:785–813.
- Investigatory Powers Act. (c.25) (2016). London: The Stationery Office. <http://www.legislation.gov.uk/ukpga/2015/25/contents/enacted>.

- Korb, K. B. and Nicholson, A. E. (2010). *Bayesian Artificial Intelligence, Second Edition*. CRC Press, Inc., Boca Raton, FL, USA, 2nd edition.
- Krebs, V. (2002). Mapping networks of terrorist cells. *Connections*, 24.
- Leonelli, M. and Smith, J. Q. (2015). Bayesian decision support for complex systems with many distributed experts. *Annals of Operations Research*, 235(1):517–542.
- London (2019). Discussions with the counter-terrorism authorities.
- Meter, K. (2002). Terrorists/liberators: Researching and dealing with adversary social networks¹. *Connections*, 24.
- Morselli, C. (2009). *Inside criminal networks*, volume 8. Springer.
- Parveen, N. and Walker, A. (2020). Brother of manchester arena bomber found guilty of murder. *The Guardian Newspaper*.
- Pearl, J. (1988). *Probabilistic Reasoning in Intelligent Systems*. Morgan Kaufman.
- Queen, C. and Smith, J. (1993). Multiregression dynamic models. *J. Royal Statistical Society. Series B*, 55(4).
- Ranciati, S., Vinciotti, V., and Wit, E. C. (2017). Identifying overlapping terrorist cells from the Noordin Top actor-event network. *arXiv e-prints*, page arXiv:1710.10319.
- Remmers, J. M. (2019). Temporal dynamics in covert networks: A case study of the structure behind the paris and brussels attacks. *Terrorism and Political Violence*, 0(0):1–24.
- Rubin, D. B. (1976). Inference and missing data. *Biometrika*, 63(3):581–592.
- Sabbagh, D. (2020). Mi5 chief asks tech firms for ‘exceptional access’ to encrypted messages. *The Guardian Newspaper*.
- Shapiro, J. N. (2005). Organizing terror: hierarchy and networks in covert organizations. In *annual meeting of the American Political Science Association, Marriott Wardman Park, Omni Shoreham, Washington Hilton, Washington, DC*.
- Shenvi, A. and Smith, J. Q. (2019). A bayesian dynamic graphical model for recurrent events in public health. working paper.
- Smith, J. (1979). A generalization of the bayesian steady forecasting model. *Journal of the Royal Statistical Society. Series B*, 41.
- Smith, J. and Freeman, G. (2010). Distributional kalman filters for bayesian forecasting and closed form recurrences. *J. of Forecasting*, 30(1).

- Smith, J. Q. (1981). The multiparameter steady model. *Journal of the Royal Statistical Society. Series B (Methodological)*, 43(2):256–260.
- Smith, J. Q. (2010). *Bayesian decision analysis : principles and practice*. Cambridge University Press, Cambridge, UK ; New York.
- Smith, J. Q. and Shenvi, A. (2018). Assault crime dynamic chain event graphs. working paper.
- Sparrow, M. K. (1991). The application of network analysis to criminal intelligence: An assessment of the prospects. *Social Networks*, 13(3):251 – 274.
- Toth, N., Gulys, L., Legendi, R., Duijn, P., Sloot, P., and Kampis, G. (2013). The importance of centralities in dark network value chains. *The European Physical Journal Special Topics*, 222:1413–1439.
- US Department of the Army (1948). Fundamentals of Traffic Analysis (Radio-Telegraph). *Department of the Army Technical Manual TM 32-250 and Department of the Air Force Manual AFM 100-80*.
- West, M. and Harrison, J. (1997). *Bayesian Forecasting and Dynamic Models (2Nd Ed.)*. Springer-Verlag, Berlin, Heidelberg.

Acknowledgements

This work was funded by The Alan Turing Institute Defence and Security Project G027. Jim Q. Smith was supported by the Alan Turing Institute and funded by the EPSRC [grant number EP/K03 9628/1].

A Proof of Theorem 1.

Denote by $p(\phi_{ijt} | \mathcal{F}_t^-)$ the prior distributions for ϕ_{ijt} given the past information up to time $t-1$. Using the pairwise link independence assumption, ϕ_{ijt} for each pair $\{\omega_i, \omega_j\} \in \Omega_t \times \Omega_t$ can be set independently. This allows us to write prior density of Φ_t as

$$p(\Phi_t | \mathcal{F}_t^-) = \prod_{\{\omega_i, \omega_j\} \in \Omega_t \times \Omega_t} p(\phi_{ijt} | \mathcal{F}_t^-). \quad (16)$$

With the first-order Markovianity and the output independence assumptions, the matrix U_t and the posterior of Φ_t decompose as follow

$$p(U_t | \mathcal{F}_t^-) = \prod_{\{\omega_i, \omega_j\} \in \Omega_t \times \Omega_t} p(u_{ijt} | \mathcal{F}_t^-). \quad (17)$$

$$p(\Phi_t | U_t, \mathcal{F}_t^-) = \prod_{\{\omega_i, \omega_j\} \in \Omega_t \times \Omega_t} p(\phi_{ijt} | u_{ijt}, \mathcal{F}_t^-). \quad (18)$$

For each pair $\{\omega_i, \omega_j\}$, on observing a vector u_{ijt} of information from the various channels and with the information independence assumption, ϕ_{ijt} can be updated as

$$\begin{aligned} p(\phi_{ijt} | u_{ijt}, \mathcal{F}_t^-) &\propto p(\phi_{ijt} | \mathcal{F}_t^-) p(u_{ijt} | \phi_{ijt}, \mathcal{F}_t^-) \\ &= \prod_{k=1}^m p(\phi_{ijt} | \mathcal{F}_t^-) p(s_{ijk} | \phi_{ijt}, \mathcal{F}_t^-). \end{aligned} \quad (19)$$

Thus the one step ahead forecasts can be written as

$$\begin{aligned} p(u_{ijt} | \mathcal{F}_t^-) &= \int_{\phi_{ijt}} p(u_{ijt} | \phi_{ijt}, \mathcal{F}_t^-) p(\phi_{ijt} | \mathcal{F}_t^-) d\phi_{ijt} \\ &= \prod_{k=1}^m \int_{\phi_{ijt}} p(s_{ijk} | \phi_{ijt}, \mathcal{F}_t^-) p(\phi_{ijt} | \mathcal{F}_t^-) d\phi_{ijt} \end{aligned} \quad (20)$$

Now the marginal likelihood of the first-order Markov model described by the graph \mathcal{G} can be decomposed into a product of the one step ahead forecasts as follows:

$$\begin{aligned} p(U_1, \dots, U_t | \mathcal{F}_1^-) &= \prod_{s=1}^t p(U_s | \mathcal{F}_s^-) \\ &= \prod_{s=1}^t \prod_{\{\omega_i, \omega_j\} \in \Omega_s \times \Omega_s} \prod_{k=1}^m \int_{\phi_{ijs}} p(s_{ijk} | \phi_{ijs}, \mathcal{F}_s^-) p(\phi_{ijs} | \mathcal{F}_s^-) d\phi_{ijs} \end{aligned} \quad (21)$$

or equivalently as a sum of the log marginal likelihoods as

$$\log(p(U_1, \dots, U_t | \mathcal{F}_1^-)) = \sum_{s=1}^t \sum_{\{\omega_i, \omega_j\} \in \Omega_s \times \Omega_s} \sum_{k=1}^m \log p(s_{ijk s} | \mathcal{F}_s^-) \quad (22)$$

where \mathcal{F}_1^- reflects the initial information fed into the model at time t_0 .

B Proof of Theorem 2.

Here we use the d-separation theorem for Bayesian Networks (Cowell et al., 2001; Pearl, 1988) as it applies to dynamic settings (Korb and Nicholson, 2010). Similar to the graphs in Figure 4, the graph of the IDSS can also be thought of a 2TS-DBN. The moralised version of the 2TS-DBN (IDSS) graph in Figure 5 is shown in Figure 15.

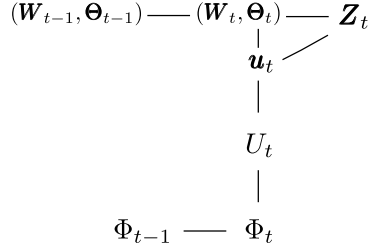


Figure 15: Moralised graph of the 2TS-DBN in Figure 5.

From the moralised graph, we can see that all the paths between (W_t, Θ_t) and Φ_t pass through U_t and u_t . Note that two variables X and Y are conditionally independent given a set of conditioning variables Z if there is no path connecting X and Y after removing the variables in Z from the moralised graph. Thus the following conditional independence relationships can be identified from the moralised graph in Figure 15.

$$(W_t, \Theta_t) \perp\!\!\!\perp \Phi_t \mid \Phi_{t-1}, (W_{t-1}, \Theta_{t-1}), U_t, Z_t$$

and

$$(W_t, \Theta_t) \perp\!\!\!\perp \Phi_t \mid \Phi_{t-1}, (W_{t-1}, \Theta_{t-1}), u_t, Z_t.$$

Assume that we have set up priors so that

$$(W_0, \Theta_0) \perp\!\!\!\perp \Phi_0,$$

and let

$$\mathcal{F}_t^1 \triangleq \{U_s, Z_s\}_{0 < s \leq t}, \quad \mathcal{F}_t^2 \triangleq \{U_s\}_{0 < s \leq t}, \quad \mathcal{F}_t^3 \triangleq \{u_s, Z_s\}_{0 < s \leq t}.$$

Now iterating forwards on the first of these equations using the semi-graphoid axioms and using the fact that observations are independent of all variables given the current realisations of its parents we obtain that for all times t that

$$(\mathbf{W}_t, \boldsymbol{\Theta}_t) \perp\!\!\!\perp \Phi_t \mid \mathcal{F}_t^1.$$

This means that given the full histories of the individuals, the states associated with the individual RVEs and the states associated with the collaboration network model remain independent.

Secondly, we note from unrolling the moralised graph and using the d-separation theorem that

$$\Phi_t \perp\!\!\!\perp \left((\mathbf{W}_t, \boldsymbol{\Theta}_t), \{\mathbf{Z}_s\}_{0 < s \leq t} \right) \mid \mathcal{F}_t^2$$

which, in particular, implies that the past data $\{\mathbf{Z}_s\}_{0 < s \leq t}$ has no effect on distributions of $\Phi_t \mid \mathcal{F}_t^2$. This means that the network model can be fully updated without having to consider $\{\mathbf{Z}_s\}_{0 < s \leq t}$ conditional on observing $\{U_s\}_{0 < s \leq t}$. In fact there is an even stronger relationship here. If we assume that whenever we observe $\{\mathbf{Z}_s\}_{0 < s \leq t}$ for a particular $\omega \in \Omega_t$ we also see the much smaller collection of measurements $\{\mathbf{u}_s\}_{0 < s \leq t}$ this modularity also holds because it represents an ancestral sample (see Smith (2010)). This will almost inevitably hold because if we observe ω 's communications we also in particular observe communications with ω 's neighbours in Ω_t which will be what is measured through the extent $\{u_s\}_{0 < s \leq t}$ path in the vector process $\{\mathbf{u}_s\}_{0 < s \leq t}$.

Thirdly, again by iterating these equations forward, we have that

$$(\mathbf{W}_t, \boldsymbol{\Theta}_t) \perp\!\!\!\perp \Phi_t \mid \mathcal{F}_t^3.$$

By conditioning on the sequence $\{\mathbf{u}_s\}_{0 < s \leq t}$ the formulae for the update of $p(\Theta_t \mid \mathcal{F}_{t-1}^3)$ are simple closed form expressions: a straightforward generalisation of those given in Bunnin and Smith (2019). This means that we can obtain means and the covariance matrices moving forward in time of the threat posed by the whole group again in closed form: see Queen and Smith (1993).

C Tables of RVE and CC model variables

| States | Tasks | Observables |
|---------------|---|---|
| Neutral | EngageWithRadicalisers | RadWebVisits |
| ActiveConvert | EngageInPublicThreats | PhysicalMeetsWithRadicals |
| Training | MakePersonalThreats | E-MeetsWithradicals |
| Preparing | AttendanceAtRadicalEventsPublic | RadicalStatementsPublic |
| Mobilised | ReducePublicEngagementsInRadicalisation | RadicalStatementsPrivate |
| | ReduceContactWithFamilyFriends | MeetTrainedRadicals |
| | Obtain Financial Resources | MeetCellMembers |
| | Travel to training camp | SeenAtRadicalDemonstrations |
| | ReconnoitreTargets | ReductionInSightingsAtRadicalDemos |
| | MoveToTargetToAttack | ReductionContactsWithNonRadicals |
| | Learn to drive | PublicThreatsMade |
| | Obtain vehicle | PersonalThreatMade |
| | Learn how to construct bomb | SellAssets |
| | Purchase bomb making materials | IncreaseInFinances |
| | Constuct bomb | DecreaseInFinances |
| | TestBomb | E-VisitsToTargetLocations |
| | Plant bomb | VisitsToTargetLocations |
| | Learn how to use gun | LegacyStatements |
| | Convert legal device to gun | StatementOfIntent |
| | Acquire Gun | GeneralCarWebSearches |
| | Acquire Ammunition | ObtainLicence |
| | Acquire knife | Driving lessons |
| | | Purchase car |
| | | Rent car |
| | | CarDealerWebHits |
| | | CarDealerPhysicalVisits |
| | | E-messages about cars |
| | | LargeExpenditure |
| | | BombMakingWebSiteHits |
| | | BombManualsBought |
| | | TechnicalElectro/ChemicalWebsiteHits |
| | | TechnicalElectro/ChemicalManualsBought |
| | | VisitsToPotentialTestingSites |
| | | Purchase of flight tickets to training countries |
| | | GunWebSearches |
| | | ShootingTrainingCourses |
| | | VisitsToGunShops |
| | | VisitsToShootingRanges |
| | | Purchase of convertible device eg CS gas pisto... |
| | | Medium to large expenditure |
| | | Stolen gun known in location |
| | | Contacts with gun and ammunition dealers |
| | | KnifeWebSearches |
| | | SeenBuyingKnives |
| | | SeenwithKnife |

Table 4: Example state space, task vector and observable data

| | $\phi_{1,2}$ | | $\phi_{1,3}$ | | $\phi_{1,4}$ | | $\phi_{2,3}$ | | $\phi_{2,4}$ | | $\phi_{3,4}$ | |
|----------|--------------|---------|--------------|---------|--------------|---------|--------------|---------|--------------|---------|--------------|---------|
| | α | β | α | β | α | β | α | β | α | β | α | β |
| t0 | 1 | 2 | | | | | 1 | 2 | | | | |
| t1prior | 0.70 | 1.41 | | | | | 0.70 | 1.41 | | | | |
| t1post | 0.70 | 2.41 | | | | | 0.70 | 2.41 | | | | |
| t2prior | 0.50 | 1.70 | | | | | 0.50 | 1.70 | | | | |
| t2post | 3.50 | 2.70 | | | | | 1.50 | 2.70 | | | | |
| t3prior | 2.46 | 1.90 | | | | | 1.05 | 1.90 | | | | |
| t3post | 7.46 | 2.90 | | | 2 | 1 | 1.05 | 2.90 | | | | |
| t4prior | 5.26 | 2.04 | | | 1.41 | 0.70 | 0.74 | 2.04 | | | | |
| t4post | 10.26 | 3.04 | | | 6.41 | 1.70 | 0.74 | 3.04 | | | | |
| t5prior | 7.23 | 2.15 | | | 4.52 | 1.20 | 0.52 | 2.15 | | | | |
| t5post | 12.23 | 3.15 | 2 | 1 | 9.52 | 2.20 | 0.52 | 3.15 | 1 | 1 | | |
| t6prior | 8.62 | 2.22 | 1.41 | 0.70 | 6.71 | 1.55 | 0.37 | 2.22 | 0.70 | 0.70 | | |
| t6post | 13.62 | 3.22 | 7.41 | 1.70 | 12.71 | 2.55 | 5.37 | 3.22 | 6.70 | 1.70 | 1 | 1 |
| t7prior | 9.60 | 2.27 | 5.22 | 1.20 | 8.95 | 1.80 | 3.78 | 2.27 | 4.72 | 1.20 | 0.70 | 0.70 |
| t7post | 16.60 | 3.27 | 11.22 | 2.20 | 15.95 | 2.80 | 9.78 | 3.27 | 11.72 | 2.20 | 7.70 | 1.70 |
| t8prior | 11.70 | 2.30 | 7.91 | 1.55 | 11.24 | 1.97 | 6.89 | 2.30 | 8.26 | 1.55 | 5.43 | 1.20 |
| t8post | 17.70 | 3.30 | 13.91 | 2.55 | 19.24 | 2.97 | 10.89 | 3.30 | 16.26 | 2.55 | 13.43 | 2.20 |
| t9prior | 12.47 | 2.33 | 9.80 | 1.80 | 13.56 | 2.09 | 7.68 | 2.33 | 11.46 | 1.80 | 9.46 | 1.55 |
| t9post | 19.47 | 3.33 | 16.80 | 2.80 | 22.56 | 3.09 | 14.68 | 3.33 | 20.46 | 2.80 | 18.46 | 2.55 |
| t10prior | 13.72 | 2.34 | 11.84 | 1.97 | 15.90 | 2.18 | 10.34 | 2.34 | 14.42 | 1.97 | 13.01 | 1.80 |
| t10post | 20.72 | 3.34 | 19.84 | 2.97 | 26.90 | 3.18 | 18.34 | 3.34 | 24.42 | 2.97 | 23.01 | 2.80 |
| t11prior | 14.60 | 2.36 | 13.98 | 2.09 | 18.95 | 2.24 | 12.93 | 2.36 | 17.21 | 2.09 | 16.22 | 1.97 |

Table 5: α , and β parameters through time for $\phi_{1,2,t}$, $\phi_{1,3,t}$, $\phi_{1,4,t}$, $\phi_{2,3,t}$, $\phi_{2,4,t}$, and $\phi_{3,4,t}$.

| | $\phi_{1,2}$ | | $\phi_{1,3}$ | | $\phi_{1,4}$ | | $\phi_{2,3}$ | | $\phi_{2,4}$ | | $\phi_{3,4}$ | |
|----------|--------------|------|--------------|------|--------------|------|--------------|------|--------------|------|--------------|------|
| | mean | std | mean | std | mean | std | mean | std | mean | std | mean | std |
| t0 | 0.50 | 0.50 | | | | | 0.50 | 0.50 | | | | |
| t1prior | 0.50 | 0.60 | | | | | 0.50 | 0.60 | | | | |
| t1post | 0.29 | 0.35 | | | | | 0.29 | 0.35 | | | | |
| t2prior | 0.29 | 0.42 | | | | | 0.29 | 0.42 | | | | |
| t2post | 1.30 | 0.69 | | | | | 0.55 | 0.45 | | | | |
| t3prior | 1.30 | 0.83 | | | | | 0.55 | 0.54 | | | | |
| t3post | 2.57 | 0.94 | | | 2 | 1.41 | 0.36 | 0.35 | | | | |
| t4prior | 2.57 | 1.12 | | | 2 | 1.68 | 0.36 | 0.42 | | | | |
| t4post | 3.37 | 1.05 | | | 3.76 | 1.49 | 0.24 | 0.28 | | | | |
| t5prior | 3.37 | 1.25 | | | 3.76 | 1.77 | 0.24 | 0.34 | | | | |
| t5post | 3.89 | 1.11 | 2 | 1.41 | 4.32 | 1.40 | 0.17 | 0.23 | 1 | 1 | | |
| t6prior | 3.89 | 1.32 | 2 | 1.68 | 4.32 | 1.67 | 0.17 | 0.27 | 1 | 1.19 | | |
| t6post | 4.23 | 1.15 | 4.35 | 1.60 | 4.98 | 1.40 | 1.67 | 0.72 | 3.93 | 1.52 | 1 | 1 |
| t7prior | 4.23 | 1.37 | 4.35 | 1.90 | 4.98 | 1.66 | 1.67 | 0.86 | 3.93 | 1.81 | 1 | 1.19 |
| t7post | 5.08 | 1.25 | 5.10 | 1.52 | 5.70 | 1.43 | 2.99 | 0.96 | 5.33 | 1.56 | 4.52 | 1.63 |
| t8prior | 5.08 | 1.49 | 5.10 | 1.81 | 5.70 | 1.70 | 2.99 | 1.14 | 5.33 | 1.85 | 4.52 | 1.94 |
| t8post | 5.36 | 1.27 | 5.45 | 1.46 | 6.48 | 1.48 | 3.30 | 1.00 | 6.37 | 1.58 | 6.10 | 1.66 |
| t9prior | 5.36 | 1.52 | 5.45 | 1.74 | 6.48 | 1.76 | 3.30 | 1.19 | 6.37 | 1.88 | 6.10 | 1.98 |
| t9post | 5.85 | 1.33 | 6.00 | 1.47 | 7.29 | 1.54 | 4.41 | 1.15 | 7.31 | 1.62 | 7.24 | 1.68 |
| t10prior | 5.85 | 1.58 | 6.00 | 1.75 | 7.29 | 1.83 | 4.41 | 1.37 | 7.31 | 1.93 | 7.24 | 2.01 |
| t10post | 6.20 | 1.36 | 6.68 | 1.50 | 8.46 | 1.63 | 5.48 | 1.28 | 8.22 | 1.66 | 8.22 | 1.71 |
| t11prior | 6.20 | 1.62 | 6.68 | 1.79 | 8.46 | 1.94 | 5.48 | 1.53 | 8.22 | 1.98 | 8.22 | 2.04 |

Table 6: Prior and posterior means, standard deviations (std) through time $\phi_{1,2,t}$, $\phi_{1,3,t}$, $\phi_{1,4,t}$, $\phi_{2,3,t}$, $\phi_{2,4,t}$, and $\phi_{3,4,t}$.